16th World Conference on Earthquake, 16WCEE 2017
Santiago Chile, January 9th to 13th 2017
Paper N° 2776
Registration Code: S-K1464561300

ON MAXIMUM EARTHQUAKE SCENARIOS OF THE TJORNES FRACTURE ZONE, NORTH ICELAND FOR SEISMIC HAZARD ASSESSMENT

M. Kowsari(1), B. Halldorsson(2)

(1) *Ph.D. Student, Earthquake Engineering Research Centre & Faculty of Civil and Environmental Engineering, School of Engineering & Natural Sciences, University of Iceland, Selfoss, Iceland. milad@hi.is*
(2) *Research Professor & Director of Research, Earthquake Engineering Research Centre. Faculty of Civil and Environmental Engineering, School of Engineering & Natural Sciences, University of Iceland, Selfoss, Iceland, skykkur@hi.is*

Abstract

The Tjornes Fracture Zone (TFZ) of North Iceland is one of the most active seismic zones in northwestern Europe. While the earthquake of 1910 with M=7.2 is the largest observed earthquake in TFZ, due to the uncertainty inherent in the Icelandic earthquake catalog at present, in addition to the limitations of the written historical annals, there does not at present exist a consensus on the maximum potential of seismic sources in the region. However, for earthquake hazard studies the maximum earthquake potential of the TFZ seismic sources, needs to be evaluated either by deterministic or probabilistic approaches. In this study we carry out the analyses to estimate the maximum magnitudes, starting by revising the TFZ earthquake catalog in order to obtain a more consistently homogeneous, accurate and complete catalog. Moreover, earthquake events attributed as dependent, such as aftershocks, have been removed. We found that for active seismic regions such as the TFZ where the main faults have been identified, deterministic approaches are a better choice. We also found that results on the basis of probabilistic approaches appear to be disproportionally influenced by the estimates of the maximum observed magnitude earthquake.

Keywords: Tjornes fracture zone; maximum magnitude; deterministic and probabilistic approaches.

1. Introduction

The success of seismic risk reduction activities depends on the precise assessment of seismic hazard. With a comprehensive and accurate knowledge about seismic hazard and seismic risk, mitigation methods can be made more effective, to optimize use of limited resources [1]. Seismic hazard analysis is a practical tool that reveals some essential information about the future ground motion at a particular site. For this purpose, there are two quantitative approaches; deterministic and probabilistic. The deterministic approach gives as a result one or more scenarios (maximum magnitude and closet distance) that represents the worst situations expected using empirical attenuation relationships. On the other hand, the current seismic design provisions and guidelines suggest different hazard levels for designing of structures and facilities, it is often more meaningful to use a probabilistic seismic hazard approach at a given site. Furthermore, uncertainty in time, location and size of future earthquakes makes this desire stronger [2]. The probabilistic analysis takes into account the ground motions from the full range of earthquake magnitudes that can occur on each seismic source to quantify the annual probability of exceedance for the parameters of interest. However, the distribution of magnitude should be bounded with maximum magnitude which is required for each source zone to avoid the inclusion of unrealistically large earthquakes [3]. Maximum magnitude, Mmax, is one of the key parameters in seismic hazard studies that have a knowledge about it is necessary for any site of concern. Same as seismic hazard analysis, deterministic and probabilistic are two accepted approaches for evaluating of maximum earthquake. In deterministic approach, Mmax obtains through empirical relationships [4]. These relationships are based on the tectonic features and geological information of interested region which is related to some parameters such as type of faulting, slip rate and fault's rupture dimensions. Much research has been devoted to study on these fields [5–13]. On the contrary, the Mmax can be estimated by earthquake catalogs and an appropriate statistical procedure, in the probabilistic approach [4]. Therefore, a complete and accurate earthquake catalog is needed to estimate the value of Mmax for a given region.

The Mid-Atlantic plate boundary between the Eurasian plate and the North American plate which crosses Iceland has caused a series of volcanic and seismic zones to this region. Kinematic models show North American plate (NW Iceland) is moving westwards at a rate of 18-22 mm/yr and Eurasian plate (SE Iceland) is also moving westwards at a rate of 0-4 mm/yr [14][15]. The plate boundary in Iceland is more complex than at a typical mid-ocean ridge due to the interaction between the ridge and the Iceland hotspot [16]. The boundary is categorized by active tectonic extensional zones (i.e. volcanic belts) and transform zones which define the regions of earthquake hazard [17]. The South Iceland Seismic Zone (SISZ) and the Tjornes Fracture Zone (TFZ) located in South and North Iceland, respectively, have been considered as two major transform zones in northwestern Europe [18]. The TFZ with an approximately 120 km long and 70 km wide is an oceanic fracture zone which has been shown in Fig. 1.

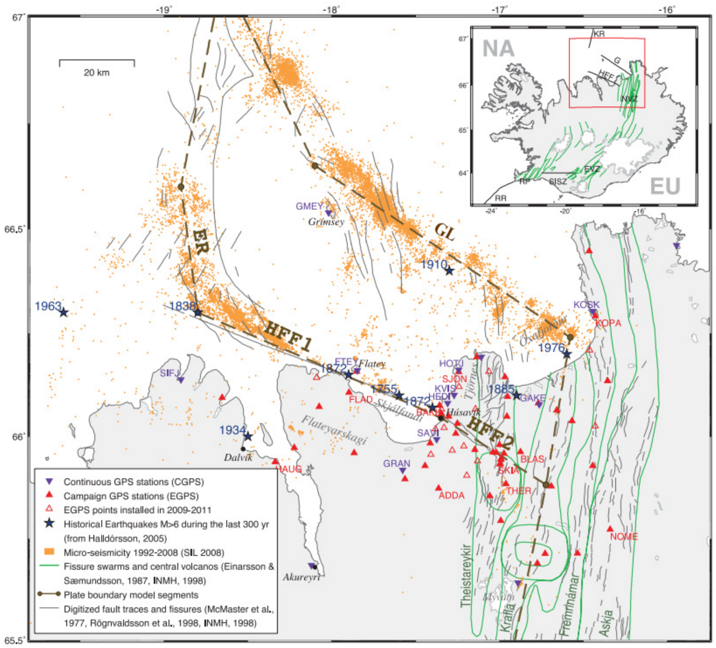

Fig. 1– The seismicity of TFZ and its major fault zones [19].

The main structural components of TFZ include two line sources, Grimsey Lineament (GL) and the Husavik–Flatey Fault (HFF). There is another lineament in this region called as Dalvik lineament (DL) which is by far less active than the HFF and GL and has not considered in this study. Currently, there are more than 140 years since a large earthquake occurred on the HFF that has been considered as the main transform structure in the TFZ and therefore a real oceanic transform fault without volcanic activities [20–22]. Historical earthquakes usually give an overall view about seismicity of the region but in Iceland, the instrumental and historical records of earthquakes are too short to reflect the full potential of the region. However, the historical events such as Ms 7 in 11 September 1755, Ms 6.5 in 12 June 1838, Ms 6.5 in 18 April 1872 and Ms 6.3 in 25 January 1885 [23–25] indicate the high seismic activity of this region. Moreover, uncertainty of the reported historical events make the estimation of maximum magnitude challenging. Therefore, in this study we evaluate the maximum potential of seismic sources in TFZ, starting by revising the TFZ earthquake catalog in order to obtain a more consistently homogeneous, accurate and complete catalog. To estimate the maximum earthquake magnitude, deterministic and probabilistic approaches are adapted through source-scaling relationships, considering earthquake catalogs and an appropriate statistical procedure, respectively.

2. Data acquisition and analysis

The earthquake catalog of Iceland like the other parts of the world can be divided into non-instrumental and instrumental data. Since instrumental earthquake observations may cover only a few decades, it is necessary to lengthen the available seismicity record using non-instrumental data [26]. The non-instrumental part of the catalog that is called as historical data, up to the beginning of the twentieth century has been collected from studies of historical sources such as annals, newspapers, letters, historic and travel books etc. According to Thorgeirsson [27], the annals are known to be the best sources of information about historical earthquakes in Iceland for the 17th and 18th century but they are not all equally good. Tryggvason et al. [28] described that 47 destructive earthquakes happened during the 1150 to 1950 in Iceland which might be incomplete especially before 1700 [23]. Whereas many of the North Iceland events had occurred off shore, they were less destructive than Southwest earthquakes which the historic sources did not mention them [27] and just five major historical events with surface-wave magnitude 6.3-7.0 [24,29] has been reported in TFZ during 1755 to 1885. Therefore, in this study the instrumental earthquakes are just used and the historical part of the catalog is ignored. The instrumental earthquakes extend from 1900 up to now, during which the development of seismographic instruments in quantity and quality. In this study, we used the TFZ catalog prepared by Ambraseys and Sigbjornsson [30] that covers the time period of 1900-1994 and also the earthquakes in 1994-2015 are gathered from the US geological survey's National Earthquake Information Center (NEIC) data-bank.

Currently, the moment magnitude (Mw) is the most reliable and important scale in engineering seismology because it can be determined from ground deformation and seismic waves, can be estimated from paleoseismological studies, is related to slip rates on faults and is also not subjected to saturation [31]. Moreover, Mw is the variable of choice for empirically and theoretically based equations for the prediction of ground motions. The catalog presented by Ambraseys and Sigbjornsson [30] is based on Ms which needs to be converted to moment magnitude. The empirical relationships are used for converting Ms to Mw [32]. Fig. 2 shows that the relationship proposed by Ambraseys and Sigbjornsson [30] fitted more better than the other relationships such as Kanamori [33], Ekstrom and Dziewonski [34] and Ambraseys and Free [35] to Icelandic earthquakes. In addition, the final collective catalog is purified from dependent shocks using the Gardner and Knopoff [36] method.

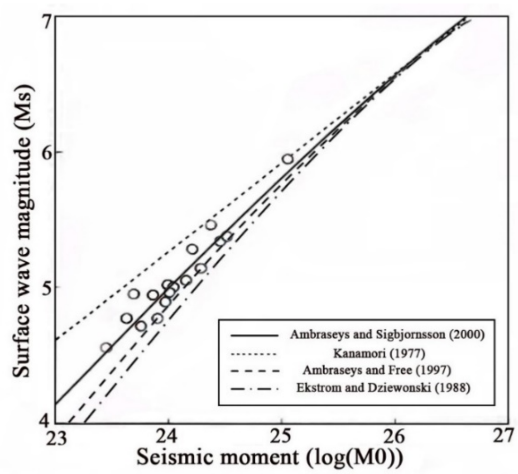

Fig. 2– Relationships between surface wave magnitude and seismic moment. The circles represent 17 Icelandic earthquakes from 1977-1994 [30].

Beside the accuracy and homogeneously of the catalog, completeness analysis should be checked as well. Completeness is a function of space and time that depicts the magnitude of the smallest events that can be reliably and completely detected. Appropriate estimation of the magnitude of completeness, Mc, is so important in seismic hazard studies because a minute change in Mc in ΔMc=0.1 leads (assuming b=1.0) to a 25% change in seismicity rates and a change of ΔMc=0.3 reduces the rate by a factor of two [37]. In this study we used three methods assuming self-similarity of the earthquake process: Entire-magnitude-range method (EMR) [37], maximum curvature-method (MAXC) [38] and goodness-of-fit test (GFT) [38]. The frequency-magnitude distribution of the TFZ catalog and the obtained Mc by EMR applied method has been shown in Fig. 3.

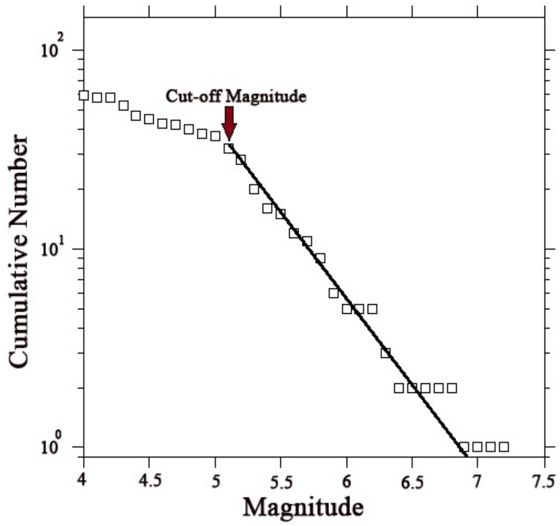

Fig. 3– The frequency-magnitude distribution along with cut-off magnitude (Mc) given by EMR method of the TFZ catalog.

3. Deterministic and probabilistic approaches

There are different types of maximum magnitudes which have their own terminologies in seismology and earthquake engineering. The upper bound of earthquake size that a seismogenic region is capable to generate it defines as maximum possible earthquake [4]. In deterministic analyses it is more common to use maximum credible earthquake that appears capable of occurring under the known tectonic framework [39]. On the other hand, maximum probable earthquake is derived using a seismic probability calculation for a recurrence within a time period [40]. Despite different terminologies and debates on what is possible, credible or probable, this discussions may be rooted more in differences of opinion with respect to the social acceptability of the facility than in differing views of earthquake potential [41]. Also, the maximum event in the region with historical or instrumental evidence calls the maximum observed earthquake. This kind of maximum magnitude most often defines the lower bound of maximum possible or maximum credible events because if the earthquake happened in the past then it is certainly possible and credible that it can happen again [41]. Source-scaling relationships not only provide an insight into the underlying mechanics of the rupture process but also give deterministic parameters for ground-motion prediction for earthquake hazard mitigation [42]. As currently practiced, researchers usually estimate magnitude-scaling relations based on various rupture and geometrical characteristics of interested seismic source. Source parameters such as rupture length, downdip rupture width, rupture area, and maximum and average displacement are commonly used to develop a series of empirical relationships for earthquakes worldwide. Among these parameters, the theoretical and empirical relations between fault rupture area and magnitude give very similar results [43]. Therefore, empirical relations giving magnitude as a function of the log of the rupture area have been found to be quite useful across the broad range of scales relevant to seismic hazard [44]. Here, we examined six magnitude-area scaling relationships to estimate Mmax. The employed relationships consist of Wells and Coppersmith [5], WC94; Somerville et al. [9], Sea99; Hanks and Bakun [10], HB02; Ellworth [45], E03; Shaw [11], Sh09 and Leonard [43], L10. It should be noted that among these equations just the equation proposed by Leonard [43] is in Newton and meter. Also, to convert seismic moment to moment magnitude Hanks and Kanamori [32] relationship is used.

On the other hand, the probabilistic approach works with earthquake catalog and statistics. With assume that the magnitudes are independent and identically distributed, the maximum possible earthquake in the region is equal to maximum observed magnitude plus a positive correction factor (Δ) where the increment Δ varies from 0.25 to 1.0 of a magnitude unit [46]. When the parametric models of the frequency-magnitude distributions are known, the parametric estimators can be used. To estimate maximum possible earthquake, three probabilistic procedures with different correction factors are used here.

3.1 Kijko-Sellevoll procedure (Cramer's approximation)

Kijko and Sellevoll [47] introduced this procedure and it has been used in several seismically active areas around the world, subsequently. In this method, Mmax can be estimated by following equation [5, 44, 45]:

$$M_{\max} = m_{\max}^{obs} + \int_{m_{\min}}^{m_{\max}} [F_M(m)]^n \, dm \tag{1}$$

where, $m_{\max}^{obs}$ is the maximum observed earthquake, n is the number of recorded magnitudes, $F_M(m)$ is cumulative distribution function for the frequency-magnitude Gutenberg-Richter relation. To solve this complicated integral, the Cramer's approximation is applied which the maximum magnitude presented in eq. (1) would be:

$$M_{\max} = m_{\max}^{obs} + \frac{E_1(n_2) - E_1(n_1)}{\beta \cdot \exp(-n_2)} + m_{\min} \exp(-n) \tag{2}$$

where, $\beta = b \ln(10)$ and b is the parameter of the Gutenberg-Richter relationship, $n_1 = n / \{1 - \exp[-\beta(m_{\max} - m_{\min})]\}$, $n_2 = n_1 \exp[-\beta(m_{\max} - m_{\min})]$ and $E_1(z)$ denotes an exponential integral function which can be approximated as $E_1(z) = \dfrac{z^2 + 2.33z + 0.25}{z(z^2 + 3.33z + 1.68)} \exp(-z)$ [5, 46]. Also the approximate variance of the estimator can be represented by:

$$Var(M_{\max}) = \sigma_M{}^2 + \left[\frac{E_1(n_2) - E_1(n_1)}{\beta \cdot \exp(-n_2)} + m_{\min} \exp(-n) \right]^2 \tag{3}$$

where, σ_M is the standard error of the maximum observed magnitude.

3.2 Kijko-Sellevoll procedure (exact solution)

It can be shown that can reach to exact solution instead of using Cramer's approximation to solve the integral in eq. (1). Therefore, Mmax and its variance can be obtained by:

$$M_{\max} = m_{\max}^{obs} + \frac{(m_{\max} - m_{\min}) + \dfrac{1}{\beta} \displaystyle\sum_{i=1}^{n} \frac{(-1)^i}{i} \binom{n}{i} (1 - \exp[-i\beta(m_{\max} - m_{\min})])}{(1 - \exp[-\beta(m_{\max} - m_{\min})])^n} \tag{4}$$

$$Var(M_{\max}) = \sigma_M^2 + \left[\frac{(m_{\max} - m_{\min}) + \dfrac{1}{\beta} \displaystyle\sum_{i=1}^{n} \frac{(-1)^i}{i} \binom{n}{i} (1 - \exp[-i\beta(m_{\max} - m_{\min})])}{(1 - \exp[-\beta(m_{\max} - m_{\min})])^n} \right]^2 \tag{5}$$

3.3 Kijko-Sellevoll-Bayes procedure

With substitution of Bayesian CDF of earthquake magnitude in (1) and after application of Cramer's approximation, the maximum possible magnitude and its variance can be expressed as:

$$M_{\max} = m_{\max}^{obs} + \frac{\delta^{1/q}\exp\left[nr^q/(1-r^q)\right]}{\beta}\left[\Gamma(-1/q,\delta r^q)-\Gamma(-1/q,\delta)\right] \quad (6)$$

$$Var(M_{\max}) = \sigma_M^2 + \frac{\delta^{1/q}\exp\left[nr^q/(1-r^q)\right]}{\beta}\left[\Gamma(-1/q,\delta r^q)-\Gamma(-1/q,\delta)\right]^2 \quad (7)$$

where, $r = p/(p+m_{\max}-m_{\min})$, $c_1 = \exp\left[-n(1-C_\beta)\right]$, $\delta = nC_\beta$, C_β is a normalizing coefficient equal to $\left\{1-\left[p/(p+m_{\max}-m_{\min})\right]^q\right\}^{-1}$, $p = \overline{\beta}/(\sigma_\beta)^2$, $q = (\overline{\beta}/\sigma_\beta)^2$ and $\Gamma(\cdot,\cdot)$ is the complementary incomplete Gamma function. The symbol $\overline{\beta}$ denotes the known mean value of the parameter β and σ_β is the known standard deviation of β. With this definition, the variation of *b*-value is presented by Gamma distribution with parameters *p* and *q* and the Bayesian distribution of $F_M(m)$ is the weighted average of the distribution of *M* for all possible values of β [46].

4. Results and Discussions

The purpose of the present study was to evaluate the maximum earthquake scenarios in TFZ by means of probabilistic and deterministic approaches. The TFZ, as one of the two main transform zones in Iceland, has two active line sources; GL and HFF. The earthquake catalog of TFZ were compiled from Ambraseys and Sigbjornsson [30] and NEIC data-bank in a rectangular area extended from 16°-20° W and 65.5°-67° N. Obviously, a suitable data sample should be accurate, homogeneous and including earthquakes over a given time period with magnitudes larger than a cut off magnitude. To have a homogeneous catalog based on Mw we used Hanks and Kanamori [32] and Ambraseys and Sigbjornsson [30] relationships. Also, the dependent shocks were purged using the variable windowing method in time and space domains proposed by Gardner and Knopoff [36]. Moreover, we used EMR, MAXC and GFT methods assuming self-similarity of the earthquake process to obtaining the Mc. The Mc and seismicity parameters, b- and a-values, have also been estimated for the region. The b-value provides information about the occurrence of an event, the magnitude distribution and the average occurrence rate of earthquakes for a given region [51] and the a-value exhibits significant variations from region to region as it depends on the level of seismic activity, the period of observation, and the length of the considered area as well as the size of earthquakes [52]. The obtained values by three applied methods are approximately same which are shown in Table 1.

Table 1 – Estimation of seismicity parameters for the TFZ by different methods

Applied method	Mc	b-value	a-value
EMR	5.1±0.20	0.86	5.93
MAXC	5.0±0.39	0.85	5.83
GFT	5.1±0.09	0.88	6.04

As currently practiced, deterministic approach uses empirical relations for various rupture and fault-based parameters to derive expected maximum magnitude. In this study, we considered six magnitude-area scaling relationships for estimating deterministic magnitude which the results are shown in Table 2. According to Metzger et al. [19], HFF is considered with two segments, HFF1 and HFF2 (Fig. 1). Based on the geological map, their length are considered to be as 82, 72 and 33 km for GL, HFF1 and HFF2, respectively. Also, we estimated the maximum magnitude for whole HFF as well which is shown in the last column of Table 2. The width, measured along the dip of the fault plane may be computed from the thickness of the seismogenic zone, H, divided on the average dip of the fault plane as measured from the horizontal plane [53]. Wright et al. [54] estimated that globally, seismogenic thickness to be 14 ± 5 and 14 ± 7 km from coseismic and interseismic observations, respectively. We considered this value equal to be 15 km for TFZ which is consistent with the Agustsson and Flovenz [55] results for this region.

Table 2– The estimated Mmax using the deterministic approach in TFZ

Equation name	Equation	Estimated Values			
		GL	HFF1	HFF2	HFF
WC94	$M = 3.98 + 1.02 \times \log A$	7.13	7.07	6.73	7.24
Sea99	$M = 3.95 + \log A$	7.04	6.98	6.64	7.14
HB02	$M = \begin{cases} 3.98 + \log A & A \le 537 km^2 \\ 3.07 + \frac{4}{3}\log A & A > 537 km^2 \end{cases}$	7.19	7.11	6.67	7.33
E03	$M = 4.2 + \log A$	7.29	7.23	6.89	7.39
Sh09	$M = 3.98 + \log A + \frac{2}{3}\log \frac{\max(1, \sqrt{\frac{A}{H^2}})}{[1 + \max(1, \frac{A}{H^2 \times 6.9})]/2}$	7.31	7.24	6.79	7.45
L10*	$\log(M_0) = 6.09 + 1.5 \times \log A$	7.15	7.09	6.75	7.25

M: moment magnitude, *A*: fault area (km^2), *H*: seismogenic depth, M_0: seismic moment, *L10 equation is in Newton and meter

The Kijko-Sellevoll (Cramer's approximation) (KS-C), Kijko-Sellevoll (Exact solution) (KS-E) and Kijko-Sellevoll-Bayes (KSB) procedures are used to estimate Mmax by the probabilistic approach. The exact distribution of the largest earthquake magnitude is replaced by its Cramér's approximation in KS-C procedure but in the KS-E procedure exact solution of Cooke's [56] generic equation is applied. It is therefore able to provide a better solution, particularly when the number of observations is limited. Also, KSB which is based on Bayes theory are useful when only a rough knowledge of the functional form of earthquake magnitude distribution is available [46]. These procedures need seismicity parameters such as rate of earthquake occurrence, maximum observed magnitude, b-value, magnitude of completeness and number of events for each seismic source. However, in TFZ is hard to distinguish the earthquake events for each causative fault, therefore, the different methods are applied for entire region as an area source. Fig. 4 shows the mean value of maximum possible earthquake and its standard deviations for KS-C, KS-E and KSB methods where the obtained results are close together.

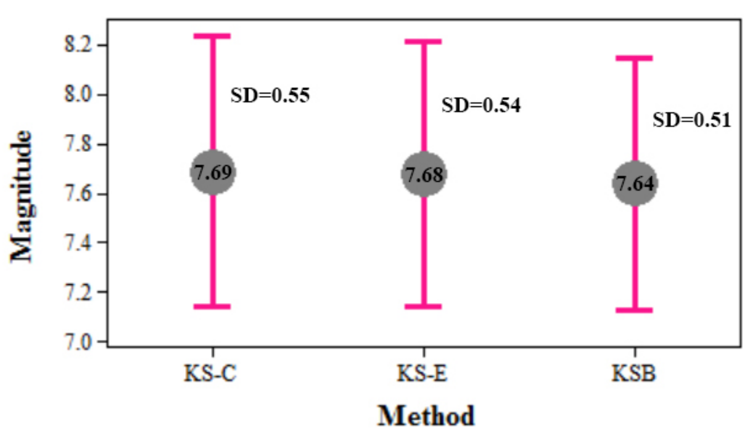

Fig. 4– Maximum posible earthquakes and its standard deviations in TFZ

The epistemic uncertainties in seismic hazard analysis may be found in the characteristics of the seismic sources, seismicity parameters (e.g., rate of occurrence, b value and maximum magnitude) and median value of ground motion. Due to existence of the uncertainty in empirical relationships and the input parameters, different approaches and relationships are used in this study. The epistemic uncertainty can be simply depicted using a logic tree which organizes one's thinking with respect to the uncertain input and also it helps in communicating assignments to others [57]. Although the use of logic trees is generally associated with probabilistic seismic hazard analysis, the method can equally be applied to deterministic approach [58]. Assigning weights for each branch of logic tree is still a challenging issue [59] and we are not going to address here, however, some factors such as robustness of the relationship, relationship's acceptancy and locality, quality and quantity of the data used and engineering judgment indeed, should be considered to make a decision.

The earthquake history, seismicity, fault slip rates, the GPS measurement and fault trenching all can be used to assess future activity of seismic sources where incomplete understandings about it might lead to wrong assessment of the hazard for area under study. Usually, seismic sources may be characterized as line and area sources. The line source is defined as the projection of the fault on the ground surface and in case of the faults are not identifiable then seismic sources may be described by areal which has an uniform seismic potential. As we have shown, the deterministic approach is able to simply estimate the maximum magnitude as the worst-case scenario for a given line source. On the other hand, probabilistic methods can be useful for area sources or regions with sparse information which a good example of such a region was the 26 December 2003 Mw=6.5 Bam earthquake, southeast Iran, that the causative fault of this catastrophic event had not previously been identified [60]. Therefore, both deterministic and probabilistic methods could be useful in different situations but we suggest the deterministic approach for active seismic regions such as the TFZ where the main faults have been identified. Metzger et al. [21] through calculation of the accumulated seismic moment using the fault slip rate, the shear modulus and the total potential rupture area declared that if all accumulated moment since the last big event would be released in one large earthquake on the HFF, its moment magnitude could reach Mw=6.8 ± 0.1. The probabilistic results are far away from the physical models obtained by Metzger et al. [56] because the probabilistic results appear to be disproportionally influenced by the estimates of the maximum observed magnitude which is a historical event with uncertainty in TFZ earthquake catalog.

5. Acknowledgements

This study was funded by Grant of Excellence (No. 141261-051) from the Icelandic centre for research which is gratefully acknowledged. The authors would like to express their sincere gratitude to Prof. Andrzej Kijko for providing his computer code.

6. References

[1] Olsen MJ, Chen Z, Hutchinson T, Kuester F (2013) Optical techniques for multiscale damage assessment. *Geomatics, Natural Hazards and Risk* **4**, 49–70.

[2] Somerville P, Moriwaki Y (2003) 65 Seismic hazards and risk assessment in engineering practice. *International Geophysics* **81**, 1065–1080.

[3] Wheeler RL (2009) *Methods of Mmax estimation east of the Rocky Mountains*, US Geological Survey.

[4] Kijko A (2004) Estimation of the maximum earthquake magnitude, m max. *Pure and Applied Geophysics* **161**, 1655–1681.

[5] Wells DL, Coppersmith KJ (1994) New empirical relationships among magnitude, rupture length, rupture width, rupture area, and surface displacement. *Bulletin of the seismological Society of America* **84**, 974–1002.

[6] Anderson JG, Wesnousky SG, Stirling MW (1996) Earthquake size as a function of fault slip rate. *Bulletin of the Seismological Society of America* **86**, 683–690.

[7] Stein RS, Hanks TC (1998) M≧ 6 earthquakes in southern California during the twentieth century: No evidence for a seismicity or moment deficit. *Bulletin of the Seismological Society of America* **88**, 635–652.

[8] Field EH, Jackson DD, Dolan JF (1999) A mutually consistent seismic-hazard source model for southern California. *Bulletin of the Seismological Society of America* **89**, 559–578.

[9] Somerville P, Irikura K, Graves R, Sawada S, Wald D, Abrahamson N, Iwasaki Y, Kagawa T, Smith N, Kowada A (1999) Characterizing crustal earthquake slip models for the prediction of strong ground motion. *Seismological Research Letters* **70**, 59–80.

[10] Hanks TC, Bakun WH (2002) A bilinear source-scaling model for M-log A observations of continental earthquakes. *Bulletin of the Seismological Society of America* **92**, 1841–1846.

[11] Shaw BE (2009) Constant stress drop from small to great earthquakes in magnitude-area scaling. *Bulletin of the Seismological Society of America* **99**, 871–875.

[12] Shaw BE (2013) Earthquake Surface Slip-Length Data is Fit by Constant Stress Drop and is Useful for Seismic Hazard Analysis. *Bulletin of the Seismological Society of America* **103**, 876–893.

[13] Leonard M (2010) Earthquake fault scaling: self-consistent relating of rupture length, width, average displacement, and moment release. *Bulletin of the Seismological Society of America* **100**, 1971–1988.

[14] Müller RD, Roest WR, Royer J-Y (1998) Asymmetric sea-floor spreading caused by ridge–plume interactions. *Nature* **396**, 455–459.

[15] Angelier J, Slunga R, Bergerat F, Stefansson R, Homberg C (2004) Perturbation of stress and oceanic rift extension across transform faults shown by earthquake focal mechanisms in Iceland. *Earth and Planetary Science Letters* **219**, 271–284.

[16] Árnadóttir T, Lund B, Jiang W, Geirsson H, Björnsson H, Einarsson P, Sigurdsson T (2009) Glacial rebound and plate spreading: results from the first countrywide GPS observations in Iceland. *Geophysical Journal International* **177**, 691–716.

[17] Halldorsson B, Sigbjörnsson R (2009) The Mw6. 3 Ölfus earthquake at 15: 45 UTC on 29 May 2008 in South Iceland: ICEARRAY strong-motion recordings. *Soil Dynamics and Earthquake Engineering* **29**, 1073–1083.

[18] Bessason B, Kaynia AM (2002) Site amplification in lava rock on soft sediments. *Soil dynamics and Earthquake engineering* **22**, 525–540.

[19] Metzger S, Jónsson S, Danielsen G, Hreinsdottir S, Jouanne F, Giardini D, Villemin T (2013) Present kinematics of the Tjörnes Fracture Zone, North Iceland, from campaign and continuous GPS measurements. *Geophysical Journal International* **192**, 441–455.

[20] Gudmundsson A (2007) Infrastructure and evolution of ocean-ridge discontinuities in Iceland. *Journal of Geodynamics* **43**, 6–29.

[21] Metzger S, Jónsson S, Geirsson H (2011) Locking depth and slip-rate of the Húsavík Flatey fault, North Iceland, derived from continuous GPS data 2006-2010. *Geophysical Journal International* **187**, 564–576.

[22] Rögnvaldsson ST, Guðmundsson Á, Slunga R (1998) Seismotectonic analysis of the Tjörnes Fracture Zone, an active transform fault in north Iceland. *Journal of Geophysical Research: Solid Earth (1978–2012)* **103**, 30117–30129.

[23] Tryggvason E (1973) Seismicity, earthquake swarms, and plate boundaries in the Iceland region. *Bulletin of the Seismological Society of America* **63**, 1327–1348.

[24] Halldórsson P (2005) Jarskjálftavirkni á Norurlandi-Earthquake activity in N-Iceland. *Greinarger. Veurstofu Íslands, IMO report* **5021**, 34.

[25] Stefansson R, Gudmundsson GB, Halldorsson P (2008) Tjörnes fracture zone. New and old seismic evidences for the link between the North Iceland rift zone and the Mid-Atlantic ridge. *Tectonophysics* **447**, 117–126.

[26] Mäntyniemi P, Tatevossian RE, Tatevossian TN (2014) Uncertain historical earthquakes and seismic hazard: theoretical and practical considerations. *Geomatics, Natural Hazards and Risk* **5**, 1–6.

[27] Thorgeirsson O (2012) *Sögulegir jarðskjálftar á Norðurlandi*, Husavik Academic Centre, Husavik, Iceland.

[28] Tryggvason E, Thoroddsen S, Thorarinsson S (1958) Report on earthquake risk in Iceland. *Timarit Verkfraedingafelags Islands* **43**, 81–97.

[29] Stefansson R, Gudmundsson GB, Halldorsson P (2008) Tjörnes fracture zone. New and old seismic evidences for the link between the North Iceland rift zone and the Mid-Atlantic ridge. *Tectonophysics* **447**, 117–126.

[30] Ambraseys NN, Sigbjörnsson R (2000) Re-appraisal of the seismicity of Iceland. *Acta Polytechnica Scandinavica* **2000-003**, 1–184.

[31] Boore DM (2003) Simulation of Ground Motion Using the Stochastic Method. *Pure appl. geophys.* **160**, 635–676.

[32] Hanks TC, Kanamori H (1979) A moment magnitude scale. *Journal of Geophysical Research B* **84**, 2348–2350.

[33] Kanamori H (1977) The energy release in great earthquakes. *Journal of geophysical research* **82**, 2981–2987.

[34] Ekström G, Dziewonski AM (1988) Evidence of bias in estimations of earthquake size.

[35] Ambraseys NN, Free MW (1997) Surface-wave magnitude calibration for European region earthquakes. *Journal of Earthquake Engineering* **1**, 1–22.

[36] Gardner JK, Knopoff L (1974) Is the sequence of earthquakes in southern California, with aftershocks removed, Poissonian. *Bull. Seismol. Soc. Am* **64**, 1363–1367.

[37] Woessner J, Wiemer S (2005) Assessing the quality of earthquake catalogues: Estimating the magnitude of completeness and its uncertainty. *Bulletin of the Seismological Society of America* **95**, 684–698.

[38] Wiemer S, Wyss M (2000) Minimum magnitude of completeness in earthquake catalogs: examples from Alaska, the western United States, and Japan. *Bulletin of the Seismological Society of America* **90**, 859–869.

[39] USCOLD (1995) Guidelines for earthquake design and evaluation of structural appurtenant to dams. *United states committee on large dams*.

[40] Krinitzsky EL (2002) How to obtain earthquake ground motions for engineering design. *Engineering Geology* **65**, 1–16.

[41] Reiter L (1991) *Earthquake hazard analysis: issues and insights*, Columbia University Press.

[42] Yen Y-T, Ma K-F (2011) Source-scaling relationship for M 4.6–8.9 earthquakes, specifically for earthquakes in the collision zone of Taiwan. *Bulletin of the Seismological Society of America* **101**, 464–481.

[43] Leonard M (2010) Earthquake fault scaling: self-consistent relating of rupture length, width, average displacement, and moment release. *Bulletin of the Seismological Society of America* **100**, 1971–1988.

[44] Shaw BE (2013) Earthquake Surface Slip-Length Data is Fit by Constant Stress Drop and is Useful for Seismic Hazard Analysis. *Bulletin of the Seismological Society of America* **103**, 876–893.

[45] Ellsworth WL (2003) Magnitude and area data for strike slip earthquakes. *US Geol. Surv. Open File Rep* 03–214.

[46] Kijko A, Singh M (2011) Statistical tools for maximum possible earthquake magnitude estimation. *Acta Geophysica* **59**, 674–700.

[47] Kijko A, Sellevoll MA (1989) Estimation of earthquake hazard parameters from incomplete data files. Part I. Utilization of extreme and complete catalogs with different threshold magnitudes. *Bulletin of the Seismological Society of America* **79**, 645–654.

[48] Pisarenko VF, Lyubushin AA, Lysenko VB, Golubeva TV (1996) Statistical estimation of seismic hazard parameters: maximum possible magnitude and related parameters. *Bulletin of the Seismological Society of America* **86**, 691–700.

[49] Kijko A, Graham G (1998) Parametric-historic procedure for probabilistic seismic hazard analysis Part I: estimation of maximum regional magnitude mmax. *Pure and Applied Geophysics* **152**, 413–442.

[50] Abramowitz M, Stegun IA (1964) *Handbook of mathematical functions: with formulas, graphs, and mathematical tables*, Courier Corporation.

[51] Bastami M, Kowsari M (2014) Seismicity and seismic hazard assessment for greater Tehran region using Gumbel first asymptotic distribution. *Structural Engineering and Mechanics* **49**, 355–372.

[52] Bayrak Y, Yilmaztürk A, Öztürk S (2005) Relationships between fundamental seismic hazard parameters for the different source regions in Turkey. *Natural Hazards* **36**, 445–462.

[53] Campbell KW (1983) Bayesian analysis of extreme earthquake occurrences. Part II. Application to the San Jacinto fault zone of southern California. *Bulletin of the Seismological Society of America* **73**, 1099–1115.

[54] Wright TJ, Elliott JR, Wang H, Ryder I (2013) Earthquake cycle deformation and the Moho: Implications for the rheology of continental lithosphere. *Tectonophysics* **609**, 504–523.

[55] Ágústsson K, Flóvenz ÓG (2005) The thickness of the seismogenic crust in Iceland and its implications for geothermal systems. In *Proceedings of the World Geothermal Congress*, pp. 24–29.

[56] Cooke P (1979) Statistical inference for bounds of random variables. *Biometrika* **66**, 367–374.

[57] McGuire RK (2004) *Seismic hazard and risk analysis*, Earthquake engineering research institute.

[58] Bommer JJ, Scherbaum F, Bungum H, Cotton F, Sabetta F, Abrahamson NA (2005) On the use of logic trees for ground-motion prediction equations in seismic-hazard analysis. *Bulletin of the Seismological Society of America* **95**, 377–389.

[59] Delavaud E, Cotton F, Akkar S, Scherbaum F, Danciu L, Beauval C, Drouet S, Douglas J, Basili R, Sandikkaya MA (2012) Toward a ground-motion logic tree for probabilistic seismic hazard assessment in Europe. *Journal of Seismology* **16**, 451–473.

[60] Talebian M, Fielding EJ, Funning GJ, Ghorashi M, Jackson J, Nazari H, Parsons B, Priestley K, Rosen PA, Walker R, others (2004) The 2003 Bam (Iran) earthquake: Rupture of a blind strike-slip fault. *Geophysical Research Letters* **31**,.